Journal of Water Process Engineering 54 (2023) 103966

Contents lists available at ScienceDirect

Journal of Water Process Engineering

journal homepage: www.elsevier.com/locate/jwpe

Removal of Cr(VI) from tanning wastewater using chitosan-SDS complexes in PEUF: Optimization and analysis via response surface methodology

Berk Köker *, Meltem Sarioglu Cebeci

Department of Environmental Engineering, Sivas Cumhuriyet University, Sivas 58140, Turkey

ARTICLE INFO

Keywords:
Hexavalent chromium
Leather
Polymer
Surfactant
Ultrafiltration

ABSTRACT

In this study, we addressed the removal of hexavalent chromium (Cr(VI)), a highly toxic and soluble anionic heavy metal, using enhanced ultrafiltration (UF). The objective was to eliminate Cr(VI) species with molecular weights beyond the retention capability of standard UF membranes and achieve their retention through the incorporation of polymers and polymer-surfactant complexes within the UF membrane. Chitosan, a cationic polymer, and sodium lauryl sulfate (SDS), an anionic surfactant, were used in this context. The Cr(VI) solution was subjected to ultrafiltration in a laboratory-scale membrane cell, and its removal was assessed spectrophotometrically. Polymer and surfactant structures were characterized using turbidity, electrical conductivity, SEM-EDX, and FTIR analyses. Experimental studies were conducted using the face-centered central composite design (CCD) of the response surface methodology (RSM) to determine optimal removal and permeate flux values, as well as to unveil the relationships between the studied factors and the resulting responses.

The results revealed that 100 % of the Cr(VI) species were removed from wastewater in the chitosan-based polymer-enhanced ultrafiltration (PEUF) study. With the chitosan-SDS complex, a removal efficiency of 98.33 % was achieved in synthetic wastewater. The PEUF study employing chitosan and the chitosan-SDS complex yielded permeate flux values of 30.73 L/h/m^2 and 53.89 L/h/m^2, respectively. The optimized conditions obtained from the models were then applied to real wastewater obtained from a leather industry tanning process. In the case of chitosan and the chitosan-SDS complex, the Cr(VI) removal efficiencies in the real wastewater were 4.40 % and 98.33 %, respectively.

1. Introduction

One of the main challenges of today is the elimination of waste resulting from industrial activities. The most significant impact of this waste is the contamination of water, which is a vital part of the life cycle, rendering it unusable. Heavy metals hold a crucial place among the many pollutants found in water. Although heavy metals are typically found in trace amounts, they can cause severe health issues for living organisms. The entry of heavy metals into the living metabolism can occur through drinking water contamination, airborne intake in areas near emission sources, or through food consumption. Thus, these toxic, non-biodegradable, and persistent heavy metals of industrial origin must be removed or recovered before release into the natural environment.

Traditional methods used for heavy metal removal include chemical precipitation [1], adsorption [2–5], electrochemical treatment techniques [6–8], and ion exchangers [9]. However, these relatively more economical methods have many shortcomings, such as the need for additional treatment of the large amount of sludge that occurs, high energy requirements, and insufficient removal in some cases. Pressure-operated membrane filtration systems have been known to be effective in heavy metal removal for years. However, heavy metal removal is only possible with nanofiltration (NF) and reverse osmosis (RO) membranes [10,11]. Nevertheless, these membranes have high operating pressures and are easily fouled and clogged. Production and operating costs are also high. Additionally, they are limited in the recovery of heavy metals that may be valuable [12–14].

Ultrafiltration (UF) membranes, which have much more permeability than NF and RO membranes, have been used by modifying the process. Two of these modifications are polymer-enhanced ultrafiltration (PEUF) and micelle-enhanced ultrafiltration (MEUF). Unlike conventional UF, both methods can retain lower molecular weight components such as heavy metals and dissolved organic compounds. Water-soluble and molecular polymers are used in PEUF, and these

* Corresponding author.
E-mail address: berkkoker@cumhuriyet.edu.tr (B. Köker).

https://doi.org/10.1016/j.jwpe.2023.103966
Received 17 April 2023; Received in revised form 16 June 2023; Accepted 20 June 2023
Available online 28 June 2023

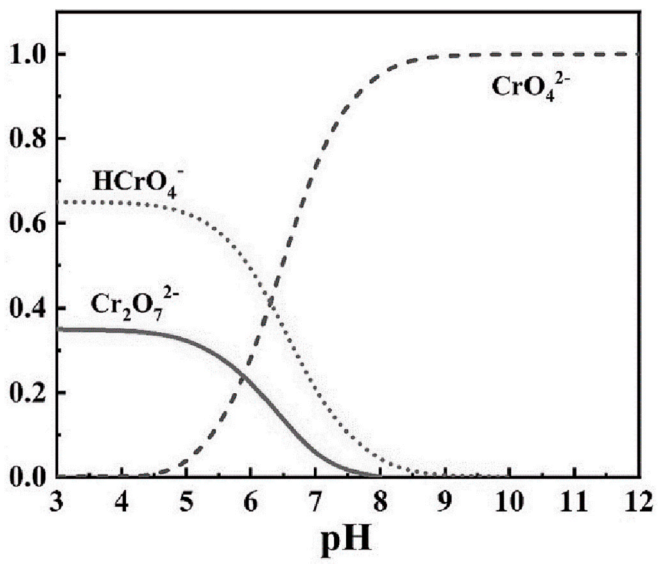

Fig. 1. Variation of Cr(VI) anions in water with respect to pH [16].

polymers interact with small-sized soluble species, increasing their total molecular weight to a size that cannot pass through UF membranes.

This study will investigate the removal of hexavalent chromium compounds with modified ultrafiltration systems. The Cr(VI) source is the chrome tanning process of the leather industry. Although Cr(III) salts are used in chrome tanning, Cr(III) can be naturally and specifically oxidized to Cr(VI). The oxidation of Cr(III) to Cr(VI) occurs when oxygen forms reactive and unstable hydrogen peroxide molecules by forming double bonds with auxiliary substances used in post-tanning processes. These radicals interact with other double bonds, triggering a free radical formation reaction. The resulting free radicals oxidize Cr(III) to Cr(VI). The reaction is catalyzed by heat and UV radiation. Unsaturated organic compounds, oils, wetting aids, and other oxidizing agents can also cause oxidation of Cr(III). The pH value applied in the neutralization stage significantly affects the formation of Cr(VI) [15–17]. Hauber [18] reports that no completely safe method exists in which hexavalent chromium is not formed. Therefore, many countries have established Cr(VI) limits for leather production, ranging from 0.5 to 50 mg/L [19–21].

Besides all of these, Cr(III) species are poorly soluble and less mobile in nature. It is an essential trace element in the metabolism of living things, including glucose, lipid, and amino acid metabolism. However, Cr(VI) is hundreds of times more toxic, water-soluble, and has high mobility. Cr(VI) has the same tetrahedral geometry as sulfates and can easily cross cell membranes. Upon contact with the skin, it causes ulcers, wounds, and eczema, while ingestion causes gastrointestinal disorders and destruction of red blood cells. Therefore, it is a much more significant environmental problem than Cr(III) [22–24].

Cr(VI) can be found in different forms in natural or effluent waters. In the pH range of 6–14, Cr(VI) is usually in the form of the dissolved chromate (CrO_4^{2-}) anion. Above pH 8, there is only CrO_4^{2-}. When the pH drops slightly below 5, it is found in the form of hydrogen chromate ($HCrO_4^-$) and Dichromate (CrO_7^{2-}). CrO_7^{2-} is the dimer of $HCrO_4^-$ and exists when the concentration rises above 1 g/L. When pH goes below 2, H_2CrO_4 is the dominant species. The pH dependent variation of certain Cr(VI) species in the aquatic environment is given in Fig. 1 [16].

The concept of polymer-enhanced ultrafiltration (PEUF) involves the use of water-soluble polymers with relatively large molecular weights that interact with dissolved small molecules, thus retaining them in the UF membrane. The primary application of this concept was for the separation of metal ions from aqueous solutions using polychaetas and UF membranes. Although there are many names for this process, such as liquid-phase polymer-assisted separation, polyelectrolyte-enhanced ultrafiltration, and polymer-assisted ultrafiltration, they all have the same basic separation mechanism [12,13].

In most cases, there are two main interactions between polymers and metal ions: electrostatic forces and coordination bonds. Other effects such as hydrogen bonds, van der Waals forces, and entrapment during aggregation or encapsulation by the polymer can also occur. The coordination bonds are similar to the interaction of metal ions with ligands in aqueous solutions. In the formation of the complex, vacant orbital metal ions function as electron acceptors, and free electron pair ligands act as electron donors, forming a coordination covalent bond. In polymer-metal coordination, macromolecular ligands are usually multidentate or have more than one metal ion attached to a single macromolecule. However, the mechanism is much more complex, as different functional groups on the polymer can interact differently [13,25].

In the first part of this study, chitosan was used as the polymer. Chitosan is a cationic amino polysaccharide copolymer with various potential applications in multiple industries. It is obtained by deacetylation of chitin, which is extracted from the exoskeleton of crustaceans and the cell walls of fungi and yeasts. It has been reported in the literature that chitosan has a high potential for use in the sorption of heavy metals, particularly due to the presence of amino groups [26,27]. Chitosan is soluble in most diluted mineral acids, and when amino groups are protonated, they form linear cationic chains [27,28]. Chitosan has two different types of reactive groups, namely the deacetylated C-2 amine group and the hydroxyl groups on the acetylated or deacetylated C-3 and C-6 carbons (Fig. 2). The reaction occurs on amine groups in an acidic environment, where amine groups serve as adsorption sites for metals such as Cd(II), As(III), and Cr(VI) [29–31].

Amine groups can bind Cr(VI) species through electrostatic, hydrogen bond, or reduction/chelation interactions. At low pH levels, the protonated amine groups are in the form of $—NH_3^+$ or $—NH_2^+$ groups. Through strong electrostatic attraction, negatively charged Cr(VI) anions bind to positively charged amine groups. The adsorption of negatively charged Cr(VI) compounds to protonated amine groups also results in the reduction of Cr(VI) to Cr(III) due to high redox potentials. In this case, both amine groups and hydroxyl groups are effective [5].

In recent years, polymer-surfactant complexes have started to be applied in addition to PEUF and MEUF applications. In this process, it is possible to use membranes with much larger pore sizes because the size of the molecules formed is larger. Moreover, the concentration required for the formation of aggregates is greatly reduced, resulting in a decrease in operating costs and an increase in removal efficiency and operating stability. In this process, oppositely charged polymers and surfactants

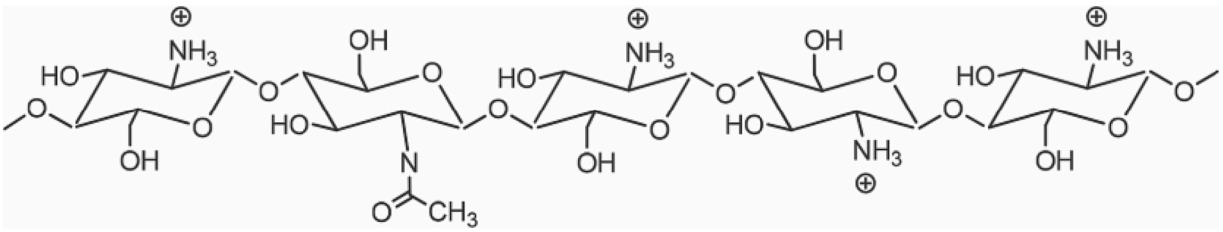

Fig. 2. Protonated polymer backbone of chitosan in acidic solution [29].

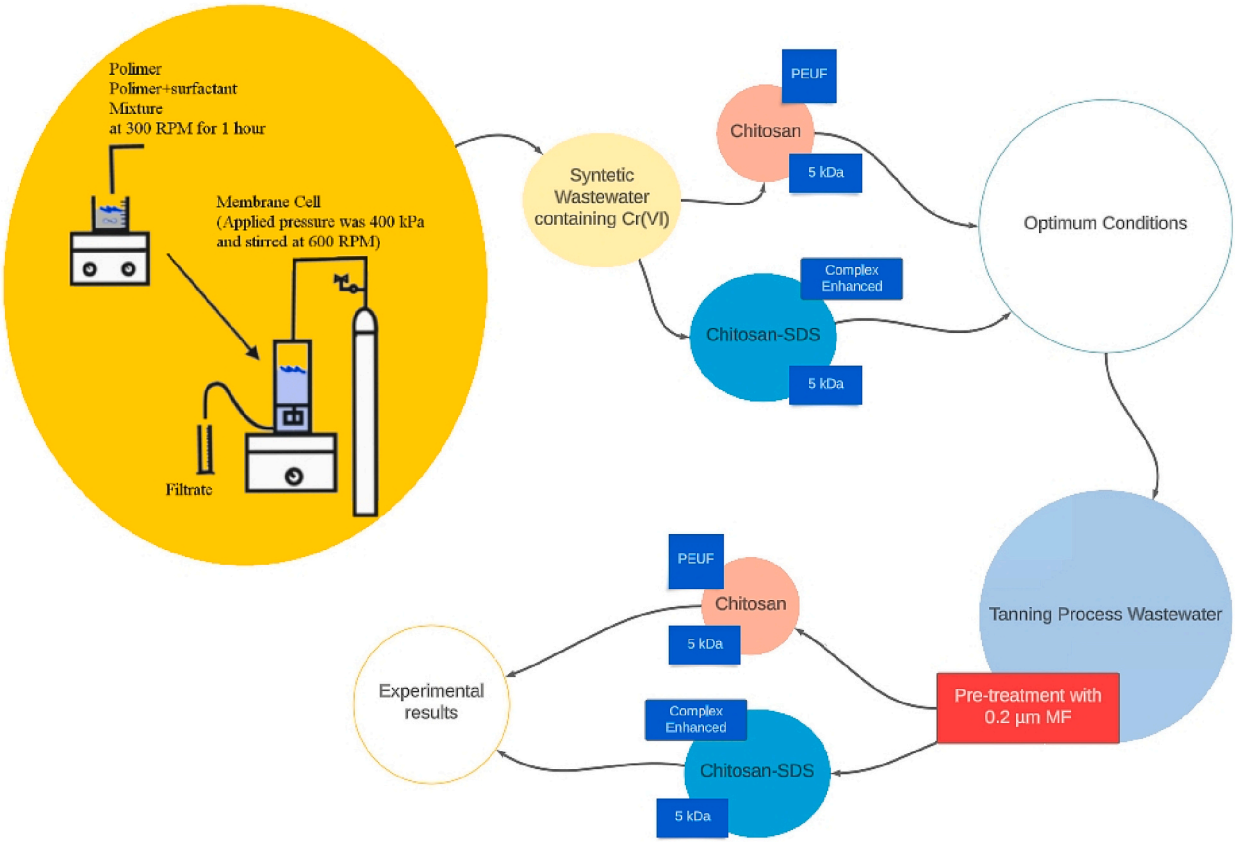

Fig. 3. Schematic representation of the experimental process.

are used, and they are typically held together by electrostatic interactions. Different interactions take place at concentrations below the critical micelle concentration (CMC), depending on the strength of the interaction between the oppositely charged surfactants and polymers. The process proceeds as follows: at low surfactant concentration, surfactant molecules are dissolved as monomers, and the surface tension decreases with increasing concentration. At moderate surfactant concentrations, surfactants begin to accumulate locally around the polymers, and the first micelle-like aggregations begin to bind to the polymer chains. The surfactant concentration at which polymer-assisted micellization begins is called the critical aggregation concentration (CAC). Surfactant added after the CAC point affects the surface tension less and allows the formation of supramolecular complexes. At this point, it should be noted that there is a break in the conductivity and surface tension slope, and turbidity starts to increase due to the presence of hydrophobic regions. Measuring the electrical conductivity of solutions containing polymer and surfactant is a frequently used method to investigate the interaction between them [32–35].

In the second part of this study, the removal of Cr(VI) will be studied using the complex formed by chitosan, a polymer, and SDS, an anionic surfactant. Chitosan has a high self-aggregation tendency due to the hydrophobicity of the polymer backbone, and it also has a low surface area since it has a non-porous structure. These properties can be eliminated by modification with SDS. SDS molecules form water-insoluble complexes by making electrostatic bonds with positively charged chitosan chains. Thus, by increasing the hydrophobicity, aggregation properties, lengths, and ionic strength of the chitosan are increased [28,31,33,36–38].

2. Material and methods

2.1. Materials

Chitosan was purchased from BLDpharm (China). Its molecular formula is $(C_6H_{11}NO_4)_n$. Acetic acid (100 % purity) was obtained from Riedel-de Haen (Germany). To prepare chitosan, a 0.1 M acetic acid solution was prepared, and chitosan was dissolved in this solution. SDS (Sodium Dodecyl Sulfate) powder was supplied from CDH (India), and its molecular formula is $CH_3(CH_2)_{11}OSO_3Na$. SDS was prepared at a concentration of 50 mM by dissolving it in distilled water. A Cr(VI) solution was prepared with pure potassium dichromate ($K_2Cr_2O_7$) in solid-state. A total of 1.2393 g of $K_2Cr_2O_7$ was dissolved in distilled water and made up to 1 L. The Cr(VI) concentration of the stock solution was 438.084 mg/L. Hydrochloric acid (HCl), and sodium hydroxide (NaOH) were purchased from Merck (Germany) and were used for pH adjustment. The membrane used is a PES membrane commercially named Microdyn Nadir UP005, which has a MWCO of 5 kDa.

2.2. Analytical methods

Cr(VI) measurements were carried out according to the methods described in APHA 3500-Cr D and DIN 38405-24. Briefly, the principle of the method is based on the reaction of Cr(VI) ions with diphenyl carbazide, resulting in the formation of a violet complex with Cr(III) in the presence of diphenyl carbazone. The Merck Spectropuant Pharo 300 UV/VIS spectrophotometer was used for Cr(VI) measurements. pH measurements were conducted using an Adwa pH/mS/EC/TDS meter. Electrical conductivity measurements were taken with the DeltaOHM HD 2106.2 conductivity meter. Turbidity measurements were obtained using the WTW TURB 355 Turbidity meter following the DIN EN 7027 standard. The critical aggregation concentration (CAC) was determined

by observing the trend of change in conductivity and turbidity values after adding SDS to the solution containing 278 mg/L chitosan at a concentration range of 0.625–20 mM. All measurements were performed at a temperature of 25 °C. FTIR analyses were carried out using the Bruker Optics Tensor II FTIR Routine Spectrometer. The FTIR spectra of the samples were determined with 16 scans at a resolution of 4 cm^{-1} in the band range of 4000–400 cm^{-1}, and the graphs were drawn using the trial version of Spectragryph v1.2.16.1. Scanning electron microscope-energy-dispersive X-ray spectroscopy (SEM-EDX) analysis was performed using the TESCAN MIRA3 XMU scanning electron microscope with an EDX detector.

2.3. Experimental process

In the study, input volume of sample was 150 cm^3. Cr(VI) solution was added to distilled water according to the concentration specified in the experimental conditions. Then, the polymer and/or surfactant were added as dropwise to the sample at concentrations based on the experimental design matrix. The pH was adjusted with addition of NaOH and HCl. The sample was stirred for 1 h in a magnetic stirrer with hotplate (WiseStir MSH-A) at 300 RPM and then transferred to the membrane cell (Sterlitech HP4750). The inlet pressure of the membrane system was adjusted, and the pressure was continuously monitored during operation. A pressure of 400 kPa (4 bar) was applied, and the sample was mixed at 600 RPM with a magnetic stirrer located under the membrane cell. The first 10 cm^3 of the filtrate was discarded, and the next 30 cm^3 was reserved for analysis. The change in flux was determined by measuring the time taken to obtain each 10 cm^3 of permeate volume. A schematic representation of the experimental process is given in Fig. 3.

The fluxes were calculated by the Eq. (1) [39]:

$$\text{Flux, F}: \quad J = \frac{\Delta V}{(A.\Delta t)} \tag{1}$$

where ΔV represent the permeate volume, A was the effective membrane area, and Δt was operation time. The result was found in L/h/m^2.

Removal efficiencies were calculated by the Eq. (2) [39]:

$$\text{Removal efficiency, R} = 1 - \frac{Cp}{Cf} \tag{2}$$

where Cp and C*f* represent pollutant concentration in the filtrate and pollutant concentration in the feed, respectively.

In order to check whether the membrane was still usable, relative permeate flux were calculated by the Eq. (3) [40]:

$$\text{Relative permeate flux} = Jr = \frac{J}{J_{H_2O}} \tag{3}$$

where JH_2O was flux of ultrapure water passed through the membrane at the beginning of the study.

2.4. Design of experiments

Design of experiment (DoE) tools and response surface methodology (RSM) provide more accurate results than the traditional experimental process in which one parameter is studied at a time and greatly reducing the number of experiments and providing data with more information. It also increases the process performance by optimizing different test conditions by revealing the interaction between the factors in the study [41]. Face-centered central composite design (CCD) was employed using Design Expert 13 (trial version) for the modeling and optimizing PEUF process. CCD usually evaluates the independent variables at 5 levels (−α, −1, 0, 1, +α). 0 is the central point. −1 and +1 are factorial points. −α and +α are called axial points or star points and represent extreme points outside the area where the model is constructed. Star points may not always conform to logical or physical work limits. These points do not have to be outside the design cube. As applied in this study, the area of interest may be close to the study area. Therefore, the star points are +1 and −1, and on the walls of the cube. It is called a face centered CCD. In face centered design, each factor must be 3 levels. It is not rotatable. Although it does not have as large a operating area as a rotatable CCD, it adequately represents the area in which the model takes place [42].

Table 1
Coded and actual experimental ranges of independent variables used in modeling Cr(VI) removal by PEUF.

Factor	Name	Units	Minimum	Maximum	Coded values	
A	pH		2	10	−1.000 = 2	1.000 = 10
B	Initial Cr (VI)	mg/L	1	5	−1.000 = 1	1.000 = 5
C	Chitosan	mg/L	0	535	−1.000 = 0	1.000 = 535

Table 2
Experimental design matrix for modeling Cr(VI) removal with PEUF.

Standard	Run	A	B	C	R1	R2
14	1	6	3	535	87.67	33.82
4	2	10	5	0	18.6	70.72
15	3	6	3	267.5	100	31.8
19	4	6	3	267.5	100	32.8
6	5	10	1	535	30	36.5
12	6	6	5	267.5	99.4	20.01
1	7	2	1	0	19	40.13
20	8	6	3	267.5	96	26.19
8	9	10	5	535	18.4	23.99
5	10	2	1	535	30	39.97
9	11	2	3	267.5	29.33	47.19
11	12	6	1	267.5	97	35.13
7	13	2	5	535	44	33.75
13	14	6	3	0	30.67	56.95
18	15	6	3	267.5	98	36.83
17	16	6	3	267.5	51	25.14
10	17	10	3	267.5	40	31.65
2	18	10	1	0	19	55.6
3	19	2	5	0	18.4	60.29
16	20	6	3	267.5	98.33	39.58

The mathematical formula of the process and the relationship between the factors and the responses are described by the quadratic Eq. (4) [43]:

$$Y = \beta_0 + \sum_{i=1}^{k} \beta_i X_i + \sum_{i=1}^{k} \beta_{ii} X_i^2 + \sum_{1 \le i \le j}^{k} \beta_{ij} X_i X_j + \varepsilon \tag{4}$$

Here, *Y* is the dependent variable, β_0 is the constant term, βi is the coefficient of linear parameters, X_i and X_j is the independent variables, βii is the coefficients of the quadratic parameters, βij is the coefficients of the interaction parameters, and ε is the random error term.

3. Results and discussion

3.1. Cr(VI) removal with chitosan-enhanced UF

In the first part of the study, chitosan solution prepared by dissolving 1 g of chitosan in 0.1 M acetic acid was used. This solution was stirred at 60 °C for 24 h and stored at 4 °C. In the experimental design, pH was coded as (A), initial Cr(VI) concentration coded as (B), and chitosan concentration (mg/L) coded as (C). The responses were Cr(VI) removal efficiency, % (R1) and permeate flux, L/h/m^2 (R2). Coded and actual values were given in Table 1. The experimental design matrix suggested for the face centered CDD model and the data obtained were given in Table 1. Coded and actual experimental ranges of independent variables used in modeling Cr(VI) removal by PEUF Table 2.

Table 3
ANOVA results of the quadratic model for Cr(VI) removal efficiency (%) with PEUF.

	Sum of squares	df	Mean square	F-Value	p-Value	
Model	0.050	4	0.012	35.68	<0.0001	Significant
A-pH	2.979E−004	1	2.979E−004	0.85	0.3711	
C-Chitosan	6.178E−003	1	6.178E−003	17.64	0.0008	
A^2	0.014	1	0.014	39.24	<0.0001	
C^2	4.583E−003	1	4.583E−003	13.08	0.0025	
Residual	5.255E−003	15	3.503E−004			
Lack of fit	3.969E−003	10	3.969E−004	1.54	0.3304	Not significant
Pure error	1.286E−003	5	2.573E−004			
Cor total	0.055	19				
R-squared	0.9049					
Adj. R-squared	0.8795					
Pred. R-squared	0.8076					
Adeq. precision	14.286					

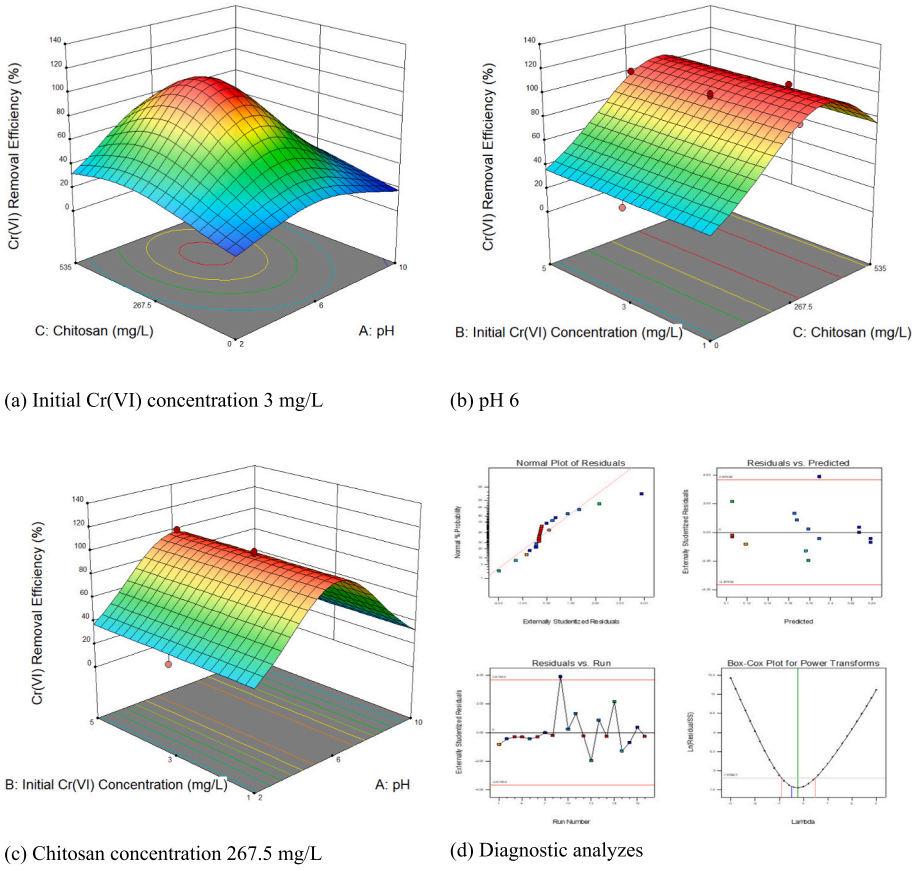

(a) Initial Cr(VI) concentration 3 mg/L

(b) pH 6

(c) Chitosan concentration 267.5 mg/L

(d) Diagnostic analyzes

Fig. 4. Response surface and contour plots of the effect of pH, chitosan concentration and initial Cr(VI) concentration on Cr(VI) removal efficiency in the PEUF with chitosan.

3.1.1. Cr(VI) removal efficiency

The ANOVA results for Cr(VI) removal efficiency with PEUF were given in Table 3. The model's F-value of 35.68 indicates that the model is significant. The *p*-value of the presented model is <0.0001, indicating that it is highly significant, and Cr(VI) removal can be explained by the independent variables. The Box-Cox graph was examined first, and it was found that lambda (λ) was −0.5. The software suggested arranging the model according to the inverse square root power law. The factors that had a limited effect on the model, with *p*-value above 0.1, were excluded. A^2, C, C^2 are significant model terms. The lack of fit F-value is 1.54. The correlation coefficient (R^2), adjusted R^2 and predicted R^2 of the model are 0.9049, 0.8795 and 0.8076, respectively. It was observed that most of the variation in the experimental data can be explained by the model, and there was compatibility between the adjusted R^2 and predicted R^2.

According to Table 3, quadratic equation of Cr(VI) removal efficiency with chitosan enhanced UF was obtained at the coded levels and given in Eq. (5):

$$1/\mathrm{Sqrt}(\mathrm{Cr(VI)\ removal\ ,\%}) = +0.11 + 5.458\mathrm{E}-003\ \mathrm{A} - 0.025\ \mathrm{C} + 0.066\ \mathrm{A}^2 + 0.038\ \mathrm{C}^2 \quad (5)$$

The response surface plots on the removal efficiency of Cr(VI) removal with PEUF were given in Fig. 4(a) as pH versus chitosan concentration. A removal efficiency exceeding 95 % was attained for hexavalent chromium (Cr(VI)) within the pH range of 4.6 to 7, utilizing a chitosan concentration ranging from approximately 270 to 450 mg/L. It was determined that the initial Cr(VI) concentration had almost no effect. Fig. 4(b) shows that at a pH of 6 and chitosan concentrations

Table 4
ANOVA results of the quadratic model for flux optimization in Cr(VI) removal with chitosan-enhanced UF.

	Sum of squares	df	Mean square	F-Value	p-Value	
Model	2949.34	6	491.56	18.73	<0.0001	Significant
A-pH	3.76	1	3.76	0.14	0.7113	
B-Initial Cr(VI) concentration	1.27	1	1.27	0.049	0.8290	
C-Chitosan	1455.88	1	1455.88	55.47	<0.0001	
AC	145.61	1	145.61	5.55	0.0349	
BC	300.25	1	300.25	11.44	0.0049	
C^2	1042.57	1	1042.57	39.72	<0.0001	
Residual	341.20	13	26.25			
Lack of fit	178.94	8	22.37	0.69	0.6957	Not significant
Pure error	162.26	5	32.45			
Cor total	3290.54	19				
R-squared	0.8963					
Adj R-squared	0.8485					
Pred R-squared	0.7804					
Adeq precision	14.820					

between 250 and 450 mg/L, a 95 % removal efficiency for Cr(VI) was achieved, and no significant effect was observed from the initial Cr(VI) concentration (Fig. 4(c)). Removal efficiency was over 95 % in the pH range of 4.8–6.8. As the pK_a value of chitosan is 6.5, some of the amino groups are protonated even at a pH of 6.9 [25,44]. The solubility of chitosan in water may also play a role. As the pH decreases, protonated chitosan becomes more soluble in water. Even if it binds Cr(VI) anions by reducing its molecular weight, it may still pass through the membrane pores. In this case, high Cr(VI) removal efficiency can be achieved in the pH range of 4.6–7, where chitosan is protonated enough to bind large molecular weight and anionic Cr(VI) compounds that will not pass through the membrane pores.

The removal of chromium is related to the presence of O- and N-containing groups. Chromate anions are bound to protonated amino groups through electrostatic attraction and ion exchange mechanisms. At this point, a redox reaction occurs between the Cr(VI) forms and amino groups, leading to the reduction of Cr(VI) to Cr(III). In addition, due to the formation of a coordination complex, immobilization occurs. At the same time, the amino groups are oxidized to —NO_2 [4,45]. Pandey and Mishra [46] suggest that the reaction may have been chelated as shown in the following reaction (Eq. (6)) [46]:

$$Cr_2O_7^{2-} + 14H^+ + 6e^- \leftrightarrow 2Cr^{3+} + 7H_2O \quad (6)$$

Li et al. [3], in their study on the production of membranes containing chitosan, determined that the highest Cr(VI) removal was achieved at pH 3. At pH 3 and below, there is competition between protons and $HCrO_4^-$. As pH increases, the protonation of anionic metal species will decrease. If pH increases to 10, there will be competition between —OH and CrO_4^{2-}. In this study, the highest removal efficiency is performed at pH 6. Zhang et al. [47] have determined that the removal efficiency decreases as the pH drops to 2. This is due to competition between protonated amino groups and anionic metal species ($HCrO_4^-$). As a result, the adsorption of $HCrO_4^-$ decreases. In addition, under strong acidic conditions, the chelation sites on chitosan decrease due to the increased protonation of —NH_2. This significantly reduces the adsorption capacity of Cr(VI), which is observed when pH is <4. Mishima et al. [48] reported that maximum retention occurred at pH 4, and also high retention of Cr(VI) also continued between pH 1–3 in their study.

3.1.2. Flux

The AVONA analysis of the reduced model, created for flux optimization in Cr(VI) removal with chitosan-enhanced UF, is presented in Table 4. As can be observed, the model is statistically significant, and there is a significant correlation within the experimental space that allows us to predict the response.

According to Table 4, quadratic equation of flux optimization in Cr (VI) removal with chitosan enhanced UF was obtained at the coded levels and given in Eq. (7):

$$\text{Flux} = +31.23 + 0.61\,A - 0.36\,B - 12.07\,C - 4.27\,AC - 6.13\,BC + 14.44\,C^2 \quad (7)$$

It is evident from the mathematical formula that chitosan concentration has a significant impact on flux, whereas the effect of pH and initial Cr(VI) concentration on flux is limited. However, the interaction between pH and chitosan, as well as initial Cr(VI) concentration and chitosan, also affect the flux. Fig. 5(a) and (b) demonstrate that flux decreases with an increase in chitosan concentration. This decrease is more pronounced at pH 10 than at pH 2. However, flux increases with decreasing chitosan concentration. It was observed that the solubility of chitosan decreased at pH 10 levels, leading to the formation of large aggregates. It is postulated that the decrease in flux is due to the formation of a layer on the membrane. At a chitosan concentration of 0 and pH of 10, the flux increased above 60 L/h/m^2.

3.1.3. Optimization

The response variables, namely Cr(VI) removal efficiency and flux, were selected to be maximized. As Cr(VI) removal efficiency is the primary objective, it was assigned a weight of +5, while the weight of flux was +1. Accordingly, the optimum solution is obtained as follows: the inlet Cr(VI) concentration is 1 mg/L, the chitosan concentration is 278 mg/L, and the pH is 5.9. Under these conditions, the removal efficiency is 100 % and the flux is 31 L/h/m^2.

3.1.4. Characterization

The chemical structure of chitosan and Cr(VI) loaded chitosan was analyzed using FTIR and SEM-EDX, and the findings are illustrated in Fig. 6. The band around 3453–3310 cm^{-1} is associated with N—H and O—H stretching vibrations. The decrease in the intensity of the broad band at 3453 cm^{-1} indicates that the O—H groups are not free. This shows that the hydroxyl groups in chitosan are one of the functional groups that form a bond with Cr(VI). The weak band at 2864 cm^{-1} is attributed to C—H stretching. The intensity of the N—H bending vibration of the free amine (—NH_2) group in the characteristic strong band at 1572 cm^{-1} is seen to decrease in the Cr(VI)-containing solution. This indicates that Cr(VI) is bound to the —NH_3^+ group in the polymer chain. The band at 1408 cm^{-1} is attributed to C—O—N deformation, while the band at 1070 cm^{-1} is attributed to C—O stretching vibration. The band in the range of 1070–1014 cm^{-1} is assigned to specific absorption peaks of the β (1–4) glucoside bond, which is a characteristic of chitosan's polysaccharide structure. The band between 900 and 670 cm^{-1} in the spectrum of the Cr(VI) solution shows strong intermolecular interactions between the polymer and Cr(VI) anions due to the shared electron cloud between them [49–56].

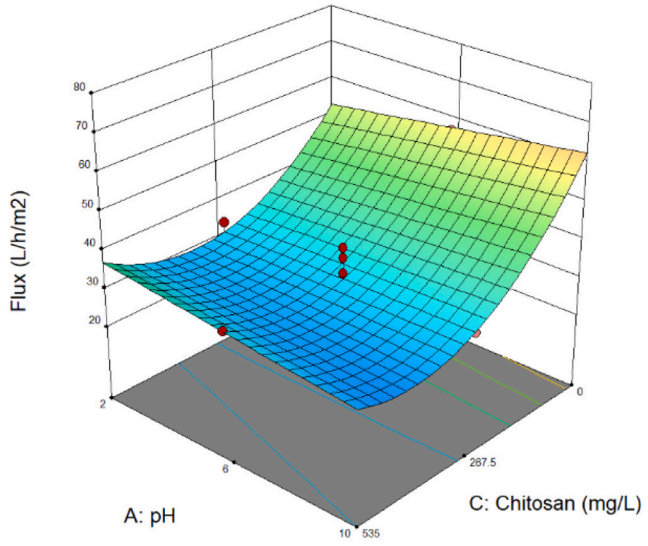

(a) Initial Cr(VI) concentration 3 mg/L

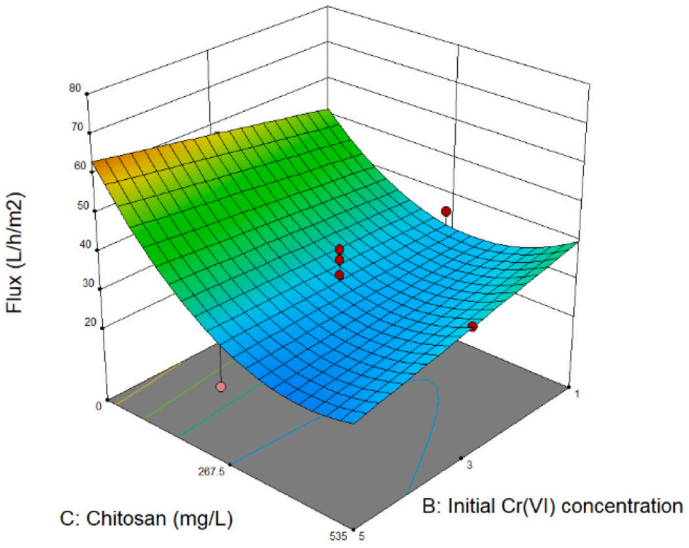

(b) pH 6

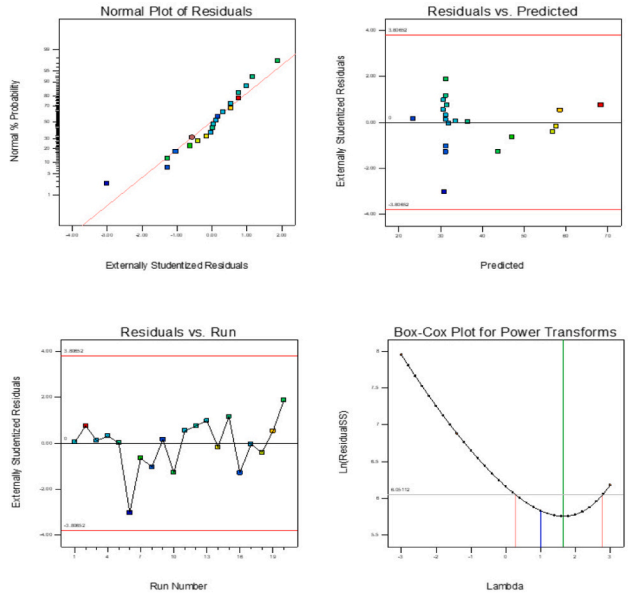

(c) Diagnostic analyzes

Fig. 5. Response surface and contour plots of the effect of pH, chitosan concentration and initial Cr(VI) concentration on flux in the chitosan-enhanced UF.

3.2. Cr(VI) removal with polymer-surfactant complex

In this section, the aim was to determine whether the complexes formed when chitosan and SDS are mixed in certain ratios in a liquid environment have an effect on the removal of Cr(VI). In a previous study, it was found that the input Cr(VI) concentration had little effect on the removal efficiency. Therefore, a fixed input Cr(VI) concentration of 3 mg/L was used in this part of the study. The factors in the experimental design were pH (coded as A), chitosan concentration in mg/L (coded as B), and SDS concentration in mM (coded as C). The responses were given as Cr(VI) removal efficiency, % (R1), and permeate flux, L/h/m^2 (R2). Coded and actual values are presented in Table 5.

The SDS concentration used in the study was determined based on the critical aggregation concentration (CAC) and critical micelle concentration (CMC). The changes in electrical conductivity (EC) and turbidity with respect to different SDS concentrations in the presence of polymer (278 mg/L chitosan) are presented graphically in Fig. 7. The CAC of 2 mM, at which SDS starts to aggregate by binding to the polymer, is clearly observed in Fig. 8. At this concentration, large and dense aggregates are formed in a core-shell structure, while less dense aggregates are formed with increasing SDS concentration [57]. As the pH increases, the number of SDS molecules that bind to chitosan decreases. A similar formation was obtained by Rasmussen et al. [57] at pH 4 and low SDS concentration.

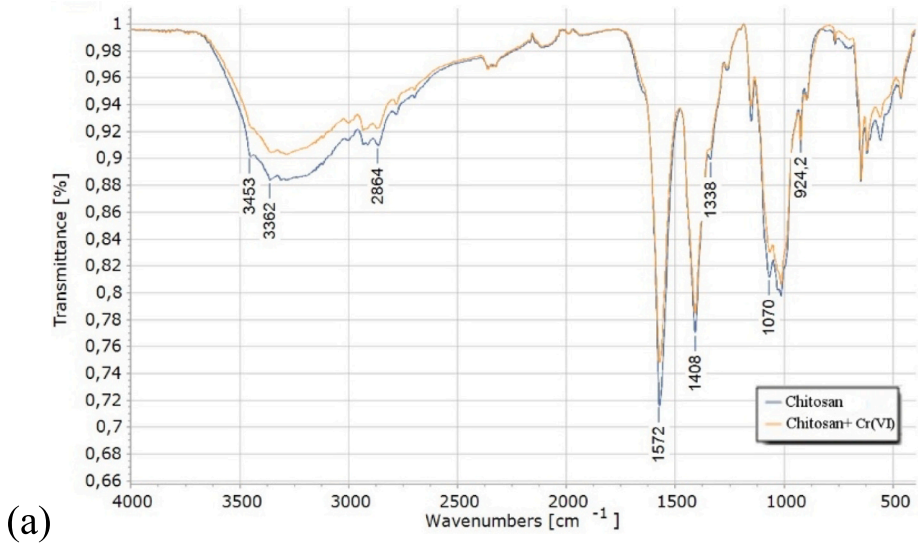

(a)

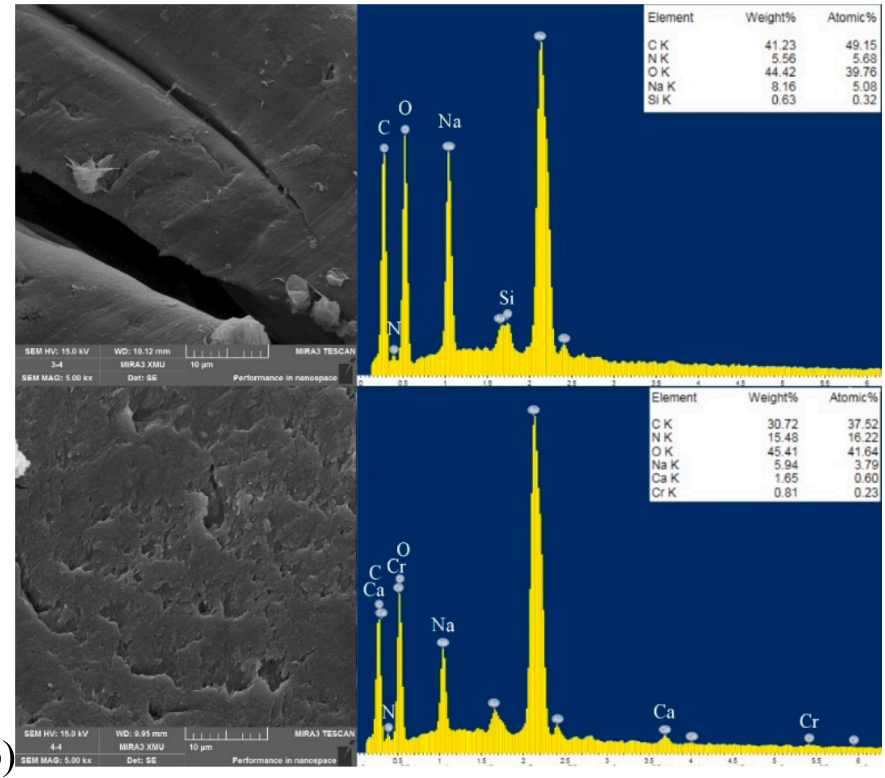

(b)

Fig. 6. FT-IR spectra (a); SEM images and EDX spectra (b) of chitosan and Cr(VI) loaded chitosan.

Table 5
Coded and actual experimental ranges of independent variables used in modeling Cr(VI) removal by PEUF.

Factor	Name	Units	Minimum	Maximum	Coded values	
A	pH		2	10	−1.000 = 2	1.000 = 10
B	Chitosan	mg/L	25	531	−1.000 = 25	1.000 = 531
C	SDS	mM	0.1	8	−1.000 = 0.1	1.000 = 8

The experimental program suggested for the face centered CDD model and the obtained data are given in Table 6.

3.2.1. *Cr(VI) removal efficiency*

The ANOVA analysis results for the Cr(VI) removal efficiency with the Chitosan-SDS complex are presented in Table 7. The F-value of the quadratic model with inverse square root transformation is 10.40 and the *p*-value associated with the F-value is 0.0003. The independent variables accurately predict the dependent variables. Model reduction was performed by eliminating the factors with limited effect on the model, with a p-value above 0.1. A, C, and C^2 are meaningful model terms. Although their *p*-values were above 0.1, the B term and the BC term, which show the chitosan-SDS interaction, were retained in the

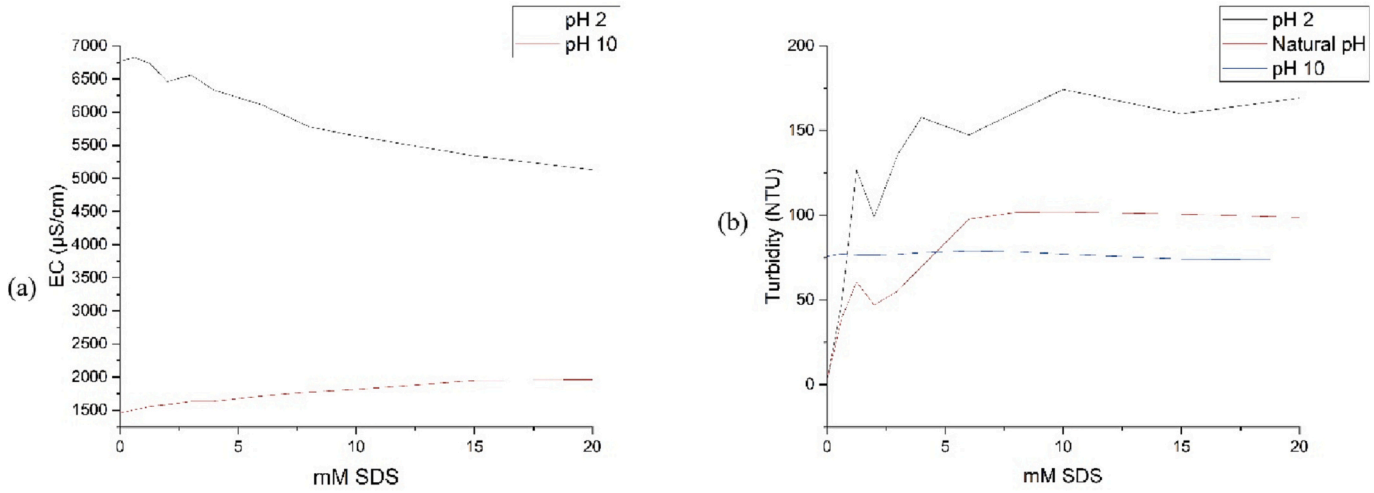

Fig. 7. EC (a) and turbidity (b) changes versus added SDS concentration at constant chitosan concentration (278 mg/L).

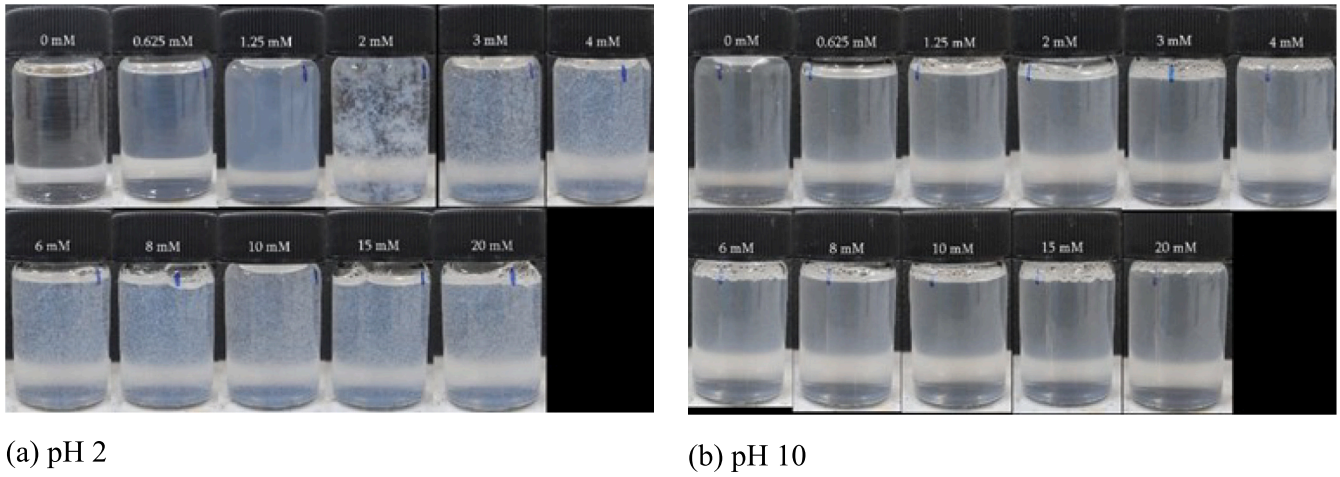

Fig. 8. Snapshots of 278 mg/L chitosan with different concentration SDS at (a) pH 2 and (b) pH 10.

model as the effect of chitosan on the model was desired to be observed. The lack of fit had an F-value of 3.21 and a p-value of 0.1058. There is a logical relationship between the variables in the current state of the model. The model R^2, adjusted R^2, and predicted R^2 values are 0.7879, 0.7121, and 0.5888, respectively. The model has sufficient sensitivity to indicate whether it is usable within the design area, which is 11.589.

Quadratic equation of Cr(VI) removal efficiency with chitosan-SDS complex was obtained at the coded levels and given in Eq. (8):

$$1/\text{Sqrt(Cr(VI) Removal efficiency)} = +0.22 - 0.027\ \text{A} - 4.078\text{E} - 003\ \text{B} + 0.016\ \text{C} + 0.013\ \text{BC} - 0.053\ \text{C}^2 \quad (8)$$

Fig. 9(a) illustrates the response surface plot when the SDS concentration is at the midpoint (4.05 mM). At this concentration, pH and chitosan concentration have little effect on the removal. However, by reducing the SDS concentration to the lowest value and increasing the pH closer to 10 (Fig. 9(b)), the removal rate increases dramatically, reaching the highest value of 98 %. A local maximum appears in Fig. 9 (c). At this point (pH 10 and SDS concentration 0.1 mM), the removal reaches the highest value. An increase in removal is also observed by increasing the SDS concentration to the highest amount. With a decrease in pH, the removal efficiency decreases to around 30–40 %. In Fig. 9(d), removal efficiency is observed at a moderate chitosan concentration (278 mg/L). At acidic pHs, the removal efficiency decreases and the effect of SDS concentration on the removal efficiency is limited. At higher pHs, the removal slightly increases as the SDS concentration rises above the CMC concentration. The removal reached the highest level at 0.01 mM SDS concentration.

3.2.2. *Flux*

The results obtained from the investigation of the effect of flux on Cr (VI) removal with chitosan-SDS complex-enhanced UF show that the amount of flux can be explained by quadratic and cubic models. When the model is cubic, an event called overfitting can occur where the model tries to predict each point instead of relating more simply and accurately to predict further data. For these reasons, the quadratic model was used, as suggested by the software. As shown in Table 8, the model is significant. The model R^2, adjusted R^2, and predicted R^2 values are 0.7833, 0.7255, and 0.7822, respectively. Model terms A, C, AC, and C^2 are significant. Within the experimental space, there is statistical relevance in predicting the response.

Equation of flux optimization in Cr(VI) removal with chitosan-SDS complex enhanced UF was obtained at the coded levels and given in Eq. (9):

$$\text{Flux} = +47.35 + 3.58\ \text{A} - 6.47\ \text{C} - 5.45\ \text{AC} - 8.97\ \text{C}^2 \quad (9)$$

In the equation that displays the effects of independent variables in the model, an increase in pH can be interpreted as an increase in flux,

Table 6
Experimental design matrix for modeling Cr(VI) removal with PEUF.

Standard	Run	A	B	C	R1	R2
17	1	6	278	4.05	19.67	51.36
5	2	2	25	8	23.67	31.53
7	3	2	531	8	23.67	33.94
9	4	2	278	4.05	17.67	45.7
6	5	10	25	8	38.33	31.13
15	6	6	278	4.05	21.33	48.3
4	7	10	531	0.1	98.33	55.98
3	8	2	531	0.1	35.67	30.52
13	9	6	278	0.1	68.67	37.17
11	10	6	25	4.05	27	44.39
10	11	10	278	4.05	40.67	42.08
1	12	2	25	0.1	23.67	42.24
2	13	10	25	0.1	37.33	58.33
8	14	10	531	8	36	32.25
14	15	6	278	8	30.33	30.67
18	16	6	278	4.05	17.33	46.05
12	17	6	531	4.05	16.33	53.6
16	18	6	278	4.05	20.33	50.32
19	19	6	278	4.05	15.67	44.93
20	20	6	278	4.05	21	46.78
21	**[21]**[a]	**10**	**531**	**0.1**	**98.67**	**54.25**

As stated in the footnote below the table, this data is different because it includes the control of a previously conducted experiment. The software used in this analysis presents the data in bold format.

[a] Control experiment of Run 7.

whereas an increase in SDS concentration can be interpreted as a decrease in flux.

The amount of flux increases as the SDS concentration decreases. The response surface plot in Fig. 10(a) shows a flat response to the variable where the chitosan concentration has no effect. This trend continues as the pH decreases. The interaction between pH and SDS concentration is more apparent in Fig. 10(b), where the highest flux values were obtained at high pH and low SDS concentrations.

3.2.3. Optimization

The response variables, Cr(VI) removal efficiency and flux, were chosen to be maximized. As Cr(VI) removal efficiency is the main objective, its weight was given as +5 and the weight of flux as +1. Under these conditions, the optimal solution was determined as follows: pH of 10, chitosan concentration of 530.98 mg/L, and SDS concentration of 0.103 mM. It was observed that a high chitosan concentration and low SDS concentration will yield the highest removal efficiency and flux in almost all solutions produced by the model.

In all other points of the experimental region, it is assumed that the amine groups on chitosan that form bonds with Cr(VI) compounds are filled by surfactant. Therefore, low Cr(VI) removal efficiency was obtained. Hassani Najafabadi et al. [58] conducted a study in which SDS was used to protect the amine groups in C2 during chitosan modification and to modify the —OH groups. Chitosan is well soluble when amine groups are protonated at low pH. However, it has low solubility at natural and high pH values. Chitosan forms aggregates and behaves like an amphiphile. SDS, on the other hand, forms strong bonds with chitosan through electrostatic attraction at low pH values. In this study, it is believed that there is no removal with the binding of SDS to protonated amine groups at low pH before Cr(VI) compounds. The mixture samples given at the beginning of the section at pH 2 and 10 also support this. Das [59] mentions the formation of strong electrostatic bonds between chitosan at high pH and low concentrations of SDS. It is thought that the negative head of SDS is turned towards the chitosan backbone. Low concentration surfactant molecules may also prevent chitosan molecular chains from clumping.

3.2.4. Characterization

The FTIR spectrum of chitosan-SDS complex is presented in Fig. 11 (a). The broad and intense peak at 3362 cm^{-1} corresponds to the stretching vibrations of the O—H and R—NH_2 groups of chitosan-SDS. It is observed that there is a significant increase in the amount of functional groups. The peak shifts from 3362 cm^{-1} to 3293 cm^{-1}, indicating a decrease in the hydrophilic character of chitosan. The peak at 2917 cm^{-1} is attributed to the aliphatic methylene group. The peak at 1556 cm^{-1} corresponds to the bending vibration of the N—H group, and the increase in its intensity indicates an increase in the adsorption of IR radiation on the functional groups. The peak at 1220 cm^{-1} is the characteristic vibration of the asymmetric C—O—S group, indicating the formation of a complex between chitosan and SDS. The peak between 950 and 800 cm^{-1} is related to the Cr—O stretching, and the decrease in the intensity of the peak at 831 cm^{-1} indicates the binding of sulfate groups. The morphology and elemental composition of the chitosan-SDS complex and chitosan-SDS loaded with Cr(VI) are given in the SEM-EDX image and spectrum in Fig. 11(b). Peaks are observed for C, N, Na, S, and Cr [2,28,31,37,49,55,58,60–63].

3.3. Treatment of chrome tanning wastewater

The optimum conditions obtained in the previous sections for synthetic wastewater treatment were used to treat the tanning process wastewater obtained from the Central Anatolian Region Mixed and Leather Industry Specialized Organized Industrial Zone in Turkey. The sample was taken from the wastewater discharged from chromium tanning and was not mixed with other process wastewaters. The wastewater was first treated as a pre-treatment by passing it through a 0.2 μm pore size MF membrane in a cross-flow membrane system. The analytical values of the obtained filtrate are given in Table 9. Due to the breakdown of aggregates in wastewater and the inadequacy of the 0.2 μm pore size MF membrane to retain Cr(VI) compounds, it is observed that the membrane filtrate becomes more concentrated in terms of Cr (VI) concentration.

Table 7
ANOVA results of the quadratic model for Cr(VI) removal efficiency (%) with Chitosan-SDS complex.

	Sum of squares	df	Mean square	F-value	p-Value	
Model	0.026	5	5.142E−003	10.40	0.0003	Significant
A-pH	−003	1	7.423E−003	15.01	0.0017	
B-Chitosan	1.663E−004	1	1.663E−004	0.34	0.5712	
C-SDS	2.647E−003	1	2.647E−003	5.35	0.0364	
BC	1.407E−003	1	1.407E−003	2.84	0.1138	
C^2	0.014	1	0.014	28.45	0.0001	
Residual	6.922E−003	14	4.944E−004			
Lack of fit	5.902E−003	9	6.557E−004	3.21	0.1058	Not significant
Pure error	1.020E−003	5	2.040E−004			
Cor total	0.033	19				
R-squared	0.7879					
Adj R-squared	0.7121					
Pred R-squared	0.5888					
Adeq precision	11.589					

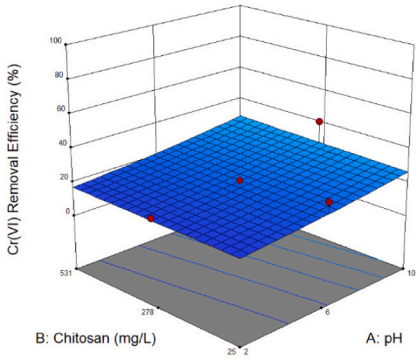

(a) SDS concentration 4.05 mM

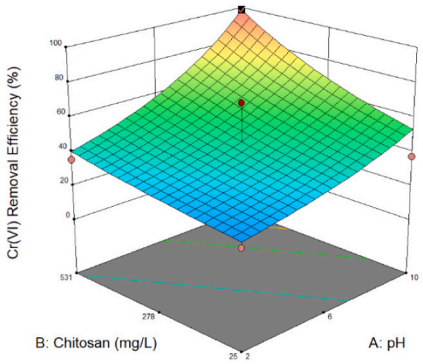

(b) SDS concentration 0.1 mM

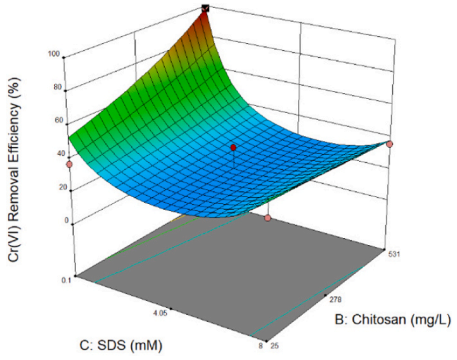

(c) pH 10

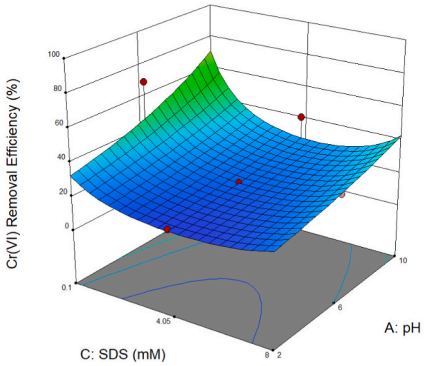

(d) Chitosan concentration 278 mg/L

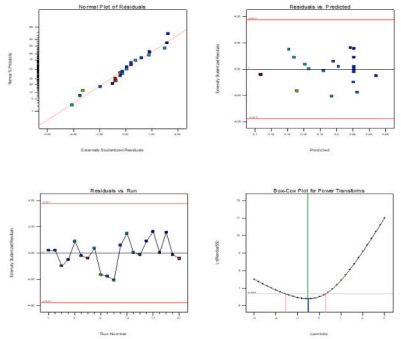

(e) Diagnostic analyzes

Fig. 9. Response surface and contour plots of the effect of pH, chitosan concentration and SDS concentration on Cr(VI) removal efficiency in the PEUF with chitosan-SDS complex.

The results obtained in the previous stages and the treatment of real wastewater are given in Table 10.

In the study that was used only chitosan, 100 % removal of Cr(VI) of synthetic water was carried out in a wide pH range and chitosan concentration. However, only 4.4 % Cr(VI) removal efficiency was obtained for real wastewater. It is believed that substances such as proteins, fats, and wetting agents, as well as competing ions present in real tannery wastewater, fill the amine and OH groups of chitosan, which form bonds with Cr(VI) [64]. By using the chitosan-SDS complex, 98.33 % Cr(VI) removal was obtained in both synthetic and real wastewater. In other words, the structure formed by chitosan and SDS can almost completely retain Cr(VI) in both synthetic wastewater and real wastewater.

In the PEUF stage with chitosan, 100 % treatment of synthetic water was achieved at a wide pH range and chitosan concentration. However, only 4.4 % removal efficiency of Cr(VI) was obtained for real wastewater. It is known that chitosan has a high chelation capacity and can form compounds with many cationic metals in addition to anions. Only alkali metals do not tend to form compounds with chitosan [12]. As an example of this situation, Kaminski et al. [65] reported that chitosan beads attracted Cu^{2+} and Zn^{2+} more than Cr(VI). Another probable reason for polymers not being able to retain Cr(VI) compounds in real wastewater may be dissolved organic compounds present in the wastewater. At the specified chitosan concentration under the experimental conditions, it is thought that the components in real wastewater fill the amine and OH functional groups of chitosan. Real wastewater could not be treated only by the PEUF with chitosan. In the section where the

Table 8
ANOVA results of the quadratic model for flux optimization in Cr(VI) removal with chitosan-SDS complex enhanced UF.

	Sum of squares	df	Mean square	F-value	p-Value	
Model	1188.13	4	297.03	13.55	<0.0001	Significant
A-pH	*128.45*	*1*	*128.45*	*5.86*	*0.0286*	
C-SDS	*418.87*	*1*	*418.87*	*19.11*	*0.0005*	
AC	*238.06*	*1*	*238.06*	*10.86*	*0.0049*	
C^2	*402.75*	*1*	*402.75*	*18.38*	*0.0006*	
Residual	328.74	15	21.92			
Lack of fit	*297.28*	*10*	*29.73*	*4.72*	*0.0502*	*Not significant*
Pure error	*31.47*	*5*	*6.29*			
Cor total	1516.87	19				
R-squared	0.7833					
Adj R-squared	0.7255					
Pred R-squared	0.5781					
Adeq precision	10.191					

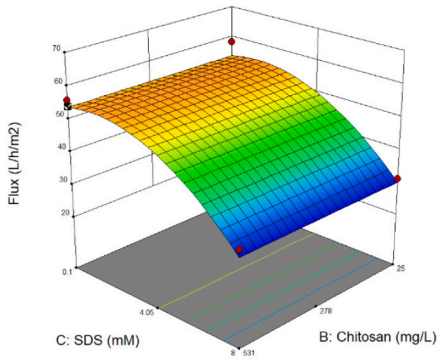

(a) pH 6

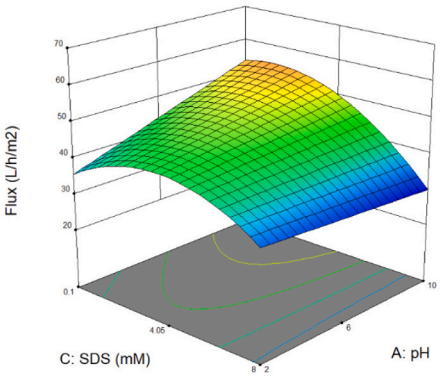

(b) Chitosan concentration 278 mg/L

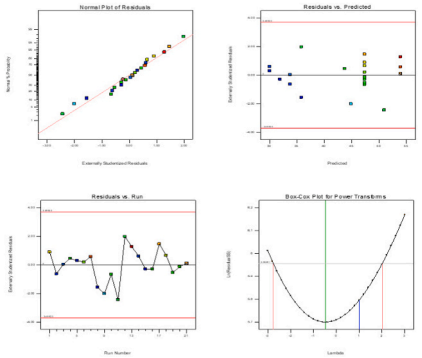

(c) Diagnostic analyzes

Fig. 10. Response surface and contour plots of the effect of pH, chitosan concentration and SDS concentration on flux in the PEUF with chitosan-SDS complex.

cationic polymer chitosan is used in combination with the anionic surfactant SDS, 99 % removal of Cr(VI) is achieved at high pH levels for synthetic wastewater. Interestingly, very low removal efficiencies were obtained in the supported UF studies using SDS and chitosan separately in the real wastewater obtained from the tanning process, whereas 98.33 % removal efficiency was achieved here. The complex formed by chitosan and SDS can almost completely adsorb both synthetic wastewater and Cr(VI) in real wastewater. The Cr(VI) concentration of the treated wastewater is below 0.05 mg/L.

4. Conclusion

The applied treatment methods in the study have provided almost complete removal of Cr(VI) compounds from both synthetic wastewater and wastewater generated from the leather industry's tanning process. In this context, Cr(VI) compounds were removed from synthetic water using the PEUF study where chitosan was used as a polymer and the UF system supported by the chitosan-SDS complex. In terms of Cr(VI) removal from real wastewater, PEUF with chitosan was not sufficient, but a remarkably high Cr(VI) removal efficiency was achieved with the UF system supported by the chitosan-SDS complex. Thus, Cr(VI) compounds that cannot be captured by UF membranes with high permeate

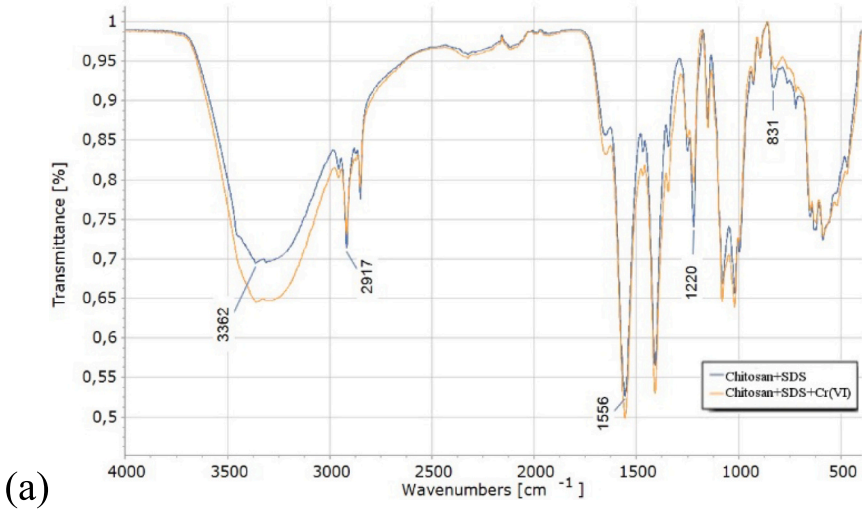

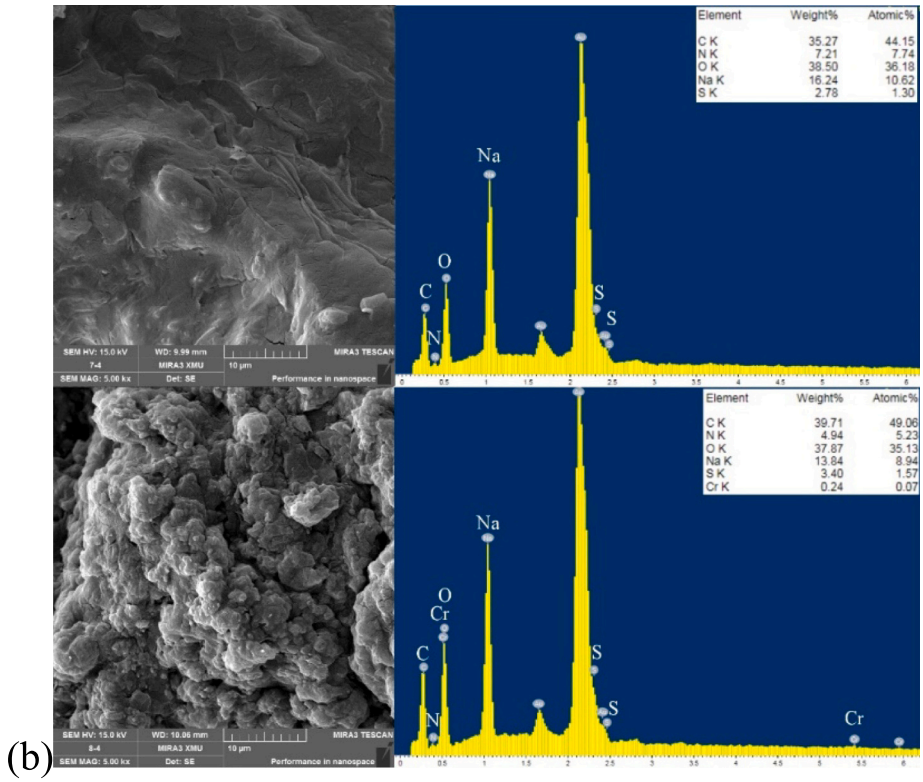

Fig. 11. FT-IR spectra (a), SEM images and EDX spectra (b) of chitosan-SDS complex and Cr(VI) loaded complex.

Table 9
The analytical values of the tanning wastewater and MF permeate.

	COD, mg/L	Cr(VI), mg/L	EC, mS/cm^2	pH
Tanning wastewater	2291.5	1.01	36.1	5.13
MF permeate	1756.3	1.86	7.56	5.46

flux were successfully captured with high efficiency in both synthetic and real wastewater, and high permeability was ensured.

Funding

This work was supported by Sivas Cumhuriyet University Scientific Research Projects (CUBAP) fund within the scope of project no M-792.

CRediT authorship contribution statement

Berk Köker: Conceptualization, Project administration, Data curation, Software, Methodology, Writing – original draft, Writing – review & editing. **Meltem Sarioglu Cebeci:** Conceptualization, Supervision, Writing – review & editing.

Declaration of competing interest

The authors declare that they have no known competing financial interests or personal relationships that could have appeared to influence the work reported in this paper.

Table 10
Results obtained in the treatment of synthetic and real wastewater with the enhanced UF membrane process.

Component I	Component II	pH	Synthetic wastewater		Tanning wastewater	
			Cr(VI) removal efficiency, %	Flux, L/h/m^2	Cr(VI) removal efficiency, %	Flux, L/h/m^2
Chitosan: 278.5 mg/L		5.86	100	30.73	4.40	41.44
Chitosan: 530.9 mg/L	SDS: 0.1 mM	10	98.33	53.89	98.33	39.41

Data availability

All data are produced by us and are clearly given in the manuscript.

References

[1] S.-Y. Pi, Y. Wang, C. Pu, X. Mao, G.-L. Liu, H.-M. Wu, H. Liu, Cr(VI) reduction coupled with Cr(III) adsorption/ precipitation for Cr(VI) removal at near neutral pHs by polyaniline nanowires-coated polypropylene filters, J. Taiwan Inst. Chem. Eng. (2021), https://doi.org/10.1016/j.jtice.2021.05.019.

[2] M. Bat-Amgalan, Z. Khashbaatar, D.E.V. Anak, M.N.M. Sari, N. Miyamoto, N. Kano, H.-J. Kim, G. Yunden, Adsorption of Cr(III) from an aqueous solution by chitosan beads modified with sodium dodecyl sulfate (SDS), J. Environ. Prot. 12 (11) (2021), 11, https://doi.org/10.4236/jep.2021.1211055.

[3] Z. Li, T. Li, L. An, P. Fu, C. Gao, Z. Zhang, Highly efficient chromium(VI) adsorption with nanofibrous filter paper prepared through electrospinning chitosan/ polymethylmethacrylate composite, Carbohydr. Polym. 137 (2016) 119–126, https://doi.org/10.1016/j.carbpol.2015.10.059.

[4] C. Lin, W. Luo, T. Luo, Q. Zhou, H. Li, L. Jing, A study on adsorption of Cr (VI) by modified rice straw: characteristics, performances and mechanism, J. Clean. Prod. 196 (2018) 626–634, https://doi.org/10.1016/j.jclepro.2018.05.279.

[5] Y.H. Yu, L. An, J.H. Bae, J.W. Heo, J. Chen, H. Jeong, Y.S. Kim, A novel biosorbent from hardwood cellulose nanofibrils grafted with poly(m-aminobenzene sulfonate) for adsorption of Cr(VI), Front. Bioeng. Biotechnol. 9 (2021). https://www.frontiersin.org/article/10.3389/fbioe.2021.682070.

[6] S. Kongjao, S. Damronglerd, M. Hunsom, Simultaneous removal of organic and inorganic pollutants in tannery wastewater using electrocoagulation technique, Korean J. Chem. Eng. 25 (4) (2008) 703–709, https://doi.org/10.1007/s11814-008-0115-1.

[7] A.N. Módenes, F.R. Espinoza-Quiñones, F.H. Borba, D.R. Manenti, Performance evaluation of an integrated photo-Fenton – electrocoagulation process applied to pollutant removal from tannery effluent in batch system, Chem. Eng. J. 197 (2012) 1–9, https://doi.org/10.1016/j.cej.2012.05.015.

[8] M. Moradi, G. Moussavi, Enhanced treatment of tannery wastewater using the electrocoagulation process combined with UVC/VUV photoreactor: parametric and mechanistic evaluation, Chem. Eng. J. 358 (2019) 1038–1046, https://doi.org/10.1016/j.cej.2018.10.069.

[9] S. Veli, B. Pekey, Removal of copper from aqueous solution by ion exchange resins, Fresenius Environ. Bull. 13 (2004) 244–250.

[10] N. Abdullah, N. Yusof, W.J. Lau, J. Jaafar, A.F. Ismail, Recent trends of heavy metal removal from water/wastewater by membrane technologies, J. Ind. Eng. Chem. 76 (2019) 17–38, https://doi.org/10.1016/j.jiec.2019.03.029.

[11] R. Shrestha, S. Ban, S. Devkota, S. Sharma, R. Joshi, A.P. Tiwari, H.Y. Kim, M. K. Joshi, Technological trends in heavy metals removal from industrial wastewater: a review, J. Environ. Chem. Eng. 9 (4) (2021), 105688, https://doi.org/10.1016/j.jece.2021.105688.

[12] G. Crini, N. Morin-Crini, N. Fatin-Rouge, S. Déon, P. Fievet, Metal removal from aqueous media by polymer-assisted ultrafiltration with chitosan, Arab. J. Chem. 10 (2017) S3826–S3839, https://doi.org/10.1016/j.arabjc.2014.05.020.

[13] Y. Huang, X. Feng, Polymer-enhanced ultrafiltration: fundamentals, applications and recent developments, J. Membr. Sci. 586 (2019) 53–83, https://doi.org/10.1016/j.memsci.2019.05.037.

[14] W. Lin, Micellar- and Polymer-enhanced Ultrafiltration for Heavy Metal and Sulfate Removal From Aqueous Solutions, Faculty of Engineering and Applied Science Memorial University of Newfoundland, 2020.

[15] K. Kolomaznik, M. Adamek, I. Andel, M. Uhlirova, Leather waste—potential threat to human health, and a new technology of its treatment, J. Hazard. Mater. 160 (2) (2008) 514–520, https://doi.org/10.1016/j.jhazmat.2008.03.070.

[16] J. Liang, X. Huang, J. Yan, Y. Li, Z. Zhao, Y. Liu, J. Ye, Y. Wei, A review of the formation of Cr(VI) via Cr(III) oxidation in soils and groundwater, Sci. Total Environ. 774 (2021), 145762, https://doi.org/10.1016/j.scitotenv.2021.145762.

[17] S.A.A. Sharaf, G.A. Gasmeleed, A.E. Musa, Reduction of hexavalent chromium from chrome shavings, Int. J. Adv. Ind. Eng. 1 (1) (2013) 24–27.

[18] C. Hauber, Formation, Prevention & Determination of Cr(VI) in Leather: A Short Overview of Recent Publications, 2000, p. 8.

[19] B. Basaran, M. Ulaş, B. Bitlisli, A. Aslan, Distribution of Cr (III) and Cr (VI) in chrome tanned leather, Indian J. Chem. Technol. 15 (2008) 511–514.

[20] J.R. Rao, P. Thanikaivelan, K.J. Sreeram, B.U. Nair, Green route for the utilization of chrome shavings (chromium-containing solid waste) in tanning industry, Environ. Sci. Technol. 36 (6) (2002) 1372–1376, https://doi.org/10.1021/es015635s.

[21] K.J. Sreeram, J. Raghava Rao, R. Sundaram, B. Unni Nair, T. Ramasami, Semi-continuous recovery of chromium from waste water, Green Chem. 2 (1) (2000) 37–41, https://doi.org/10.1039/A908916K.

[22] J.F. Cárdenas-González, I. Acosta-Rodríguez, Hexavalent chromium removal by a paecilomycessp. fungal strain isolated from environment, Bioinorganic Chem. Appl. 2010 (2010), e676243, https://doi.org/10.1155/2010/676243.

[23] X. Guo, G.T. Fei, H. Su, L. De Zhang, High-performance and reproducible polyaniline nanowire/tubes for removal of Cr(VI) in aqueous solution, J. Phys. Chem. C 115 (5) (2011) 1608–1613, https://doi.org/10.1021/jp1091653.

[24] R.M. Hassan, S.M. Ibrahim, S.A. Sayed, I.A. Zaafarany, Promising biocompatible, biodegradable, and inert polymers for purification of wastewater by simultaneous removal of carcinogenic Cr(VI) and present toxic heavy metal cations: reduction of chromium(VI) by poly(ethylene glycol) in aqueous perchlorate solutions, ACS Omega 5 (9) (2020) 4424–4432, https://doi.org/10.1021/acsomega.9b03485.

[25] S. Verbych, M. Bryk, M. Zaichenko, Water treatment by enhanced ultrafiltration, Desalination 198 (1) (2006) 295–302, https://doi.org/10.1016/j.desal.2005.12.029.

[26] R.-S. Juang, C.-H. Chiou, Ultrafiltration rejection of dissolved ions using various weakly basic water-soluble polymers, J. Membr. Sci. 177 (1) (2000) 207–214, https://doi.org/10.1016/S0376-7388(00)00464-6.

[27] G.N. Kousalya, M. Rajiv Gandhi, S. Meenakshi, Sorption of chromium(VI) using modified forms of chitosan beads, Int. J. Biol. Macromol. 47 (2) (2010) 308–315, https://doi.org/10.1016/j.ijbiomac.2010.03.010.

[28] P. Sunintaboon, K. Pumduang, T. Vongsetskul, P. Pittayanurak, N. Anantachoke, P. Tuchinda, A. Durand, One-step preparation of chitosan/sodium dodecyl sulfate-stabilized oil-in-water emulsion of Zingiber cassumunar Roxb. Oil extract, Colloids Surf. A Physicochem. Eng. Asp. 414 (2012) 151–159, https://doi.org/10.1016/j.colsurfa.2012.07.031.

[29] A. Laaraibi, F. Moughaoui, F. Damiri, A. Ouaket, I. Charhouf, S. Hamdouch, A. Jaafari, A. Abdelmjid, N. Knouzi, A. Bennamara, M. Berrada, Chitosan-Clay Based (CS-NaBNT) Biodegradable Nanocomposite Films for Potential Utility in Food and Environment, 2018, https://doi.org/10.5772/intechopen.76498.

[30] A. Aljawish, I. Chevalot, J. Jasniewski, J. Scher, L. Muniglia, Enzymatic synthesis of chitosan derivatives and their potential applications, J. Mol. Catal. B Enzym. 112 (2015) 25–39, https://doi.org/10.1016/j.molcatb.2014.10.014.

[31] X. Ren, Y. Zhang, Switching Pickering emulsion stabilized by chitosan-SDS complexes through ion competition, Colloids Surf. A Physicochem. Eng. Asp. 587 (2020), 124316, https://doi.org/10.1016/j.colsurfa.2019.124316.

[32] M. Chen, C.T. Jafvert, Y. Wu, X. Cao, N.P. Hankins, Inorganic anion removal using micellar enhanced ultrafiltration (MEUF), modeling anion distribution and suggested improvements of MEUF: a review, Chem. Eng. J. 398 (2020), 125413, https://doi.org/10.1016/j.cej.2020.125413.

[33] L. Chiappisi, M. Gradzielski, Co-assembly in chitosan–surfactant mixtures: thermodynamics, structures, interfacial properties and applications, Adv. Colloid Interf. Sci. 220 (2015) 92–107, https://doi.org/10.1016/j.cis.2015.03.003.

[34] L.C. Shen, J. Wu, S. Singh, N.P. Hankins, Removal of metallic anions from dilute aqueous solutions by polymer–surfactant aggregates, Desalination 406 (2017) 109–118, https://doi.org/10.1016/j.desal.2016.05.028.

[35] D.J.F. Taylor, R.K. Thomas, J. Penfold, Polymer/surfactant interactions at the air/water interface, Adv. Colloid Interf. Sci. 132 (2) (2007) 69–110, https://doi.org/10.1016/j.cis.2007.01.002.

[36] H. Bao, L. Li, L.H. Gan, H. Zhang, Interactions between ionic surfactants and polysaccharides in aqueous solutions, Macromolecules 41 (23) (2008) 9406–9412, https://doi.org/10.1021/ma801957v.

[37] X. Du, C. Kishima, H. Zhang, N. Miyamoto, N. Kano, Removal of chromium(VI) by chitosan beads modified with sodium dodecyl sulfate (SDS), Appl. Sci. 10 (14) (2020) Article 14, https://doi.org/10.3390/app10144745.

[38] M. Rinaudo, Chitin and chitosan: properties and applications, Prog. Polym. Sci. 31 (7) (2006) 603–632, https://doi.org/10.1016/j.progpolymsci.2006.06.001.

[39] N.H. Baharuddin, N.M. Nik Sulaiman, M.K. Aroua, Unmodified starch as water-soluble binding polymer for chromium ions removal via polymer enhanced ultrafiltration system, J. Environ. Health Sci. Eng. 12 (1) (2014) 61, https://doi.org/10.1186/2052-336X-12-61.

[40] H.M. Park, H. Oh, K.Y. Jee, Y.T. Lee, Synthesis of PVDF/MWCNT nanocomplex microfiltration membrane via atom transfer radical addition (ATRA) with enhanced fouling performance, Sep. Purif. Technol. 246 (2020), 116860, https://doi.org/10.1016/j.seppur.2020.116860.

[41] L.M.S. Pereira, T.M. Milan, D.R. Tapia-Blácido, Using response surface methodology (RSM) to optimize 2G bioethanol production: a review, Biomass Bioenergy 151 (2021), 106166, https://doi.org/10.1016/j.biombioe.2021.106166.

[42] S. Bhattacharya, Central Composite Design for Response Surface Methodology and Its Application in Pharmacy, IntechOpen, 2021, https://doi.org/10.5772/intechopen.95835.

[43] S.J.M. Breig, K.J.K. Luti, Response surface methodology: a review on its applications and challenges in microbial cultures, Mater. Today Proc. 42 (2021) 2277–2284, https://doi.org/10.1016/j.matpr.2020.12.316.

[44] Y.N. Sudhakar, M. Selvakumar, D.K. Bhat, Chapter 2—methods of preparation of biopolymer electrolytes, in: Y.N. Sudhakar, M. Selvakumar, D.K. Bhat (Eds.),

Biopolymer Electrolytes, Elsevier, 2018, pp. 35–52, https://doi.org/10.1016/B978-0-12-813447-4.00002-9.
[45] W. Wu, R. Wang, H. Chang, N. Zhong, T. Zhang, K. Wang, N. Ren, S.-H. Ho, Rational electron tunning of magnetic biochar via N, S co-doping for intense tetracycline degradation: efficiency improvement and toxicity alleviation, Chem. Eng. J. 458 (2023), 141470, https://doi.org/10.1016/j.cej.2023.141470.
[46] S. Pandey, S.B. Mishra, Organic–inorganic hybrid of chitosan/organoclay bionanocomposites for hexavalent chromium uptake, J. Colloid Interface Sci. 361 (2) (2011) 509–520, https://doi.org/10.1016/j.jcis.2011.05.031.
[47] S. Zhang, Q. Shi, G. Korfiatis, C. Christodoulatos, H. Wang, X. Meng, Chromate removal by electrospun PVA/PEI nanofibers: adsorption, reduction, and effects of co-existing ions, Chem. Eng. J. 387 (2020), 124179, https://doi.org/10.1016/j.cej.2020.124179.
[48] K. Mishima, X. Du, S. Sekiguchi, N. Kano, Experimental and theoretical studies on the adsorption and desorption mechanisms of chromate ions on cross-linked chitosan, J. Funct. Biomater. 8 (2017) 51, https://doi.org/10.3390/jfb8040051.
[49] J. Ashenhurst, Infrared spectroscopy: a quick primer on interpreting spectra, in: Master Organic Chemistry, 2016. November 23, https://www.masterorganicchemistry.com/2016/11/23/quick_analysis_of_ir_spectra/.
[50] R. Ghosh, A. Sahu, S. Pushpavanam, Removal of trace hexavalent chromium from aqueous solutions by ion foam fractionation, J. Hazard. Mater. 367 (2019) 589–598, https://doi.org/10.1016/j.jhazmat.2018.12.105.
[51] M.N.M. Ismael, A. El Nemr, E.S.H. El Ashry, H. Abdel Hamid, Removal of hexavalent chromium by cross-linking chitosan and N,N'-methylene bis-acrylamide, Environ. Process. 7 (3) (2020) 911–930, https://doi.org/10.1007/s40710-020-00447-2.
[52] X. Liu, IR Spectrum and Characteristic Absorption Bands. https://kpu.pressbooks.pub/organicchemistry/chapter/6-3-ir-spectrum-and-characteristic-absorption-bands/, 2021.
[53] T. Mayerhöfer, Wave optics in Infrared, Spectroscopy. (2021), https://doi.org/10.13140/RG.2.2.14293.55520/1.
[54] D.A. Palacio, V. Vásquez, B.L. Rivas, Chromate ion removal by water-soluble functionalized chitosan, Polym. Adv. Technol. 32 (7) (2021) 2690–2699, https://doi.org/10.1002/pat.5170.
[55] R.M. Silverstein, F.X. Webster, D.J. Kiemle, D.L. Bryce, Spectrometric Identification of Organic Compounds, Eighth edition, Wiley, 2015.
[56] D. Xuan Du, B. Xuan Vuong, Study on preparation of water-soluble chitosan with varying molecular weights and its antioxidant activity, Adv. Mater. Sci. Eng. 2019 (2019), e8781013, https://doi.org/10.1155/2019/8781013.
[57] H.Ø. Rasmussen, D.T.W. Wollenberg, H. Wang, K.K. Andersen, C.L.P. Oliveira, C. I. Jørgensen, T.J.D. Jørgensen, D.E. Otzen, J.S. Pedersen, The changing face of SDS denaturation: complexes of Thermomyces lanuginosus lipase with SDS at pH 4.0, 6.0 and 8.0, J. Colloid Interface Sci. 614 (2022) 214–232, https://doi.org/10.1016/j.jcis.2021.12.188.
[58] A. Hassani Najafabadi, M. Abdouss, S. Faghihi, Synthesis and evaluation of PEG-O-chitosan nanoparticles for delivery of poor water soluble drugs: ibuprofen, Mater. Sci. Eng. C 41 (2014) 91–99, https://doi.org/10.1016/j.msec.2014.04.035.
[59] A.K. Das, Micellar effect on the kinetics and mechanism of chromium(VI) oxidation of organic substrates, Coord. Chem. Rev. 248 (1) (2004) 81–99, https://doi.org/10.1016/j.cct.2003.10.012.
[60] N. Antony, H.B. Sherine, S. Rajendran, Inhibition and biocide actions of sodium dodecyl sulfate-Zn2+ system for the corrosion of carbon steel in chloride solution, Portugaliae Electrochim. Acta 28 (1) (2010) 1–14, https://doi.org/10.4152/pea.201001001.
[61] C.P. Johnston, M. Chrysochoou, Investigation of chromate coordination on ferrihydrite by in situ ATR-FTIR spectroscopy and theoretical frequency calculations, Environ. Sci. Technol. 46 (11) (2012) 5851–5858, https://doi.org/10.1021/es300660r.
[62] M. Rahman, Y. Ali, I. Saha, M.A. Raihan, M. Moniruzzaman, D.-Md.J. Alam, A. Deb, M. Khan, Date palm fiber as a potential as a potential low-cost adsorbent to uptake chromium (VI) from industrial wastewater, Desalin. Water Treat. 88 (2017) 169–178, https://doi.org/10.5004/dwt.2017.21402.
[63] F. Tanjung, S. Husseinsyah, H. Kamarudin, Effect of sodium dodecyl sulfate on mechanical and thermal properties of polypropylene/chitosan composites, J. Thermoplast. Compos. Mater. 26 (2013) 878–892, https://doi.org/10.1177/0892705711430430.
[64] L. Pietrelli, I. Francolini, A. Piozzi, M. Sighicelli, I. Silvestro, M. Vocciante, Chromium(III) removal from wastewater by chitosan flakes, Appl. Sci. 10 (6) (2020) 1925, https://doi.org/10.3390/app10061925.
[65] W. Kaminski, E. Tomczak, K. Jaros, Interactions of metal ions sorbed on chitosan beads, Desalination 218 (1) (2008) 281–286, https://doi.org/10.1016/j.desal.2007.02.023.